ELECTROPHYSIOLOGICAL ON AND OFF RESPONSES IN AUTOSOMAL DOMINANT OPTIC ATROPHY

Enyam Komla A. Morny[a]; Tom H. Margrain[a]; Alison M. Binns[b]; Marcela Votruba[a,c]

a- School of Optometry and Vision Sciences, Cardiff University, Cardiff

b- Division of Optometry and Visual Sciences, City University, London

c- Eye Unit, University Hospital of Wales, Cardiff

Corresponding Author: Marcela Votruba, School of Optometry and Vision Sciences, Cardiff University, Maindy Road, Cardiff CF24 4HQ, UK.

Email: votrubaM@cardiff.ac.uk

ABSTRACT

Purpose: To assess the effect of autosomal dominant optic atrophy (ADOA) on ON and OFF retinal ganglion cell (RGC) function by evaluating the ON and OFF components of the photopic negative response (PhNR).

Methods: Twelve participants from 6 families with *OPA1* ADOA and 16 age matched controls were recruited. Electrophysiological assessment involved pattern electroretinograms (PERG), focal (20º) and full-field long duration (250msec) flash ERGs using a red light emitting diode flash on a rod saturating blue background, and full-field brief (300 µsec) xenon flash ERGs using a red filter over a continuous rod saturating blue background. Amplitudes and implicit times of the ERG components were analyzed and the diagnostic potential of each electrophysiological technique was determined by generating receiver operating characteristic (ROC) curves.

Accepted 21-10-2015

Results: Mean amplitudes of the N95 and all PhNRs, except the full-field $PhNR_{ON}$, were significantly reduced in participants with ADOA ($p<0.01$). Subtraction of the group averaged focal ERG of ADOA participants from that of controls showed an equal loss in the focal $PhNR_{ON}$ and $PhNR_{OFF}$ components, while in the full-field ERG the loss in the $PhNR_{OFF}$ was greater than that in the $PhNR_{ON}$ component. The Areas Under the ROC Curve (AUC) for the focal $PhNR_{ON}$ (0.92), focal $PhNR_{OFF}$ (0.95) and full-field $PhNR_{OFF}$ (0.83), were not significantly different from that of the PERG N95 (0.99).

Conclusions: In patients with ADOA, the $PhNR_{ON}$ and $PhNR_{OFF}$ components are nearly symmetrically reduced in the long duration ERG suggesting that ON- and OFF-RGC pathways may be equally affected.

Accepted 21-10-2015

Introduction

Autosomal dominant optic atrophy (ADOA) is a hereditary optic neuropathy characterized by variable bilateral loss of vision in early childhood, optic nerve pallor, centrocoecal visual field scotoma and color vision defects [2-6]. It is the commonest hereditary optic neuropathy with a prevalence between 1 in 50,000 to 1 in 8,000 [7-12].

ADOA is caused primarily by mutations in the autosomal nuclear gene, *OPA1* [10, 13-16], a key player in mitochondrial dynamics, controlling mitochondrial fusion, amongst other key roles. Histopathological studies in humans [17, 18] and mouse models [19-22] show that ADOA is principally characterized by the degeneration of the retinal ganglion cells (RGC).

In a mouse model of ADOA, generated in our laboratory [22], the defect is first evident as a dendritic pruning of RGCs in B6:C3-*Opa1*^{Q285STOP} *Opa1* mutant mouse which appears to be ON-center specific[19, 23]. This selective vulnerability of ON-center RGCs may reflect their higher energy demands in comparison to their OFF-center counterparts, since *OPA1* mutations are thought to curtail mitochondrial energy output[19, 23]. This new finding has however not been investigated in humans with ADOA.

The functional integrity of RGCs can be evaluated by assessing the photopic negative response (PhNR) of the flash ERG. The PhNR is a negative potential seen after the b-wave in a photopic ERG elicited by a brief flash. The PhNR is believed to primarily originate from spiking activity in RGCs and their axons with contributions from amacrine cells and possible involvement of associated glial cells/astrocytes of

64 the retina [24-27]. When a long duration flash is used to evoke the ERG, the PhNR is
65 seen once after the b-wave ($PhNR_{ON}$) and again as a negative going potential after
66 the d-wave ($PhNR_{OFF}$). Furthermore, it has been demonstrated that the ERG
67 obtained in response to a long duration red flash of moderate intensity provides
68 optimal delineation of the $PHNR_{ON}$ and $PhNR_{OFF}$ components[24, 27, 28].
69
70 The brief flash PhNR is attenuated in patients with ADOA [29] and in the *Opa1*^{Q285STOP}
71 mutant mouse[30]. In the mouse model, the defect is seen prior to any changes in
72 visual acuity on optokinetic drum testing and prior to morphological changes on
73 retinal histology. This suggests that retinal connectivity may be affected before RGC
74 somal loss impacts on RGC function[23]. Thus the PhNR deficit could serve as a
75 marker for early disease. These early changes in RGC function may be reversible
76 and need to be defined as markers for targeted therapies in any forthcoming
77 therapeutic trials.
78
79 Miyata et al (2007) and Barnard et al (2011) highlight the diagnostic potential of the
80 PhNR in ADOA, however, the investigators used a brief white flash (broadband
81 stimulus) to evoke the PhNR, which provides a poor signal to noise ratio compared
82 to monochromatic stimuli[27], and cannot distinguish ON and OFF components.
83 Furthermore, the studies elicited full-field (global) PhNRs which, in contrast to the
84 focal PhNR, are less sensitive in detecting focal retinal lesions such as those seen in
85 early to moderate glaucoma [31, 32]. As ADOA results in localized centrocoecal visual
86 field defects[2], it might be expected that a focal stimulus presented to this region
87 would enhance the sensitivity of the PhNR to early disease-related changes.
88

The aim of this study was to assess the relative effect of ADOA on the $PhNR_{ON}$ and $PhNR_{OFF}$ components elicited using focal and full-field long duration red flashes on a rod suppressing blue background. An additional aim was to compare the diagnostic potential of the long duration PhNRs to responses which have previously been shown to be affected by ADOA; the full-field brief flash PhNR [29, 30] and the N95 amplitude of the pattern electroretinogram (PERG) [33], which also reflects spiking activity of the RGCs [34].

Methods

Participants

Twelve participants (aged 18 – 61 years) from six families with documented *OPA1* mutations and 16 healthy age matched controls (aged 19 – 61 years) were recruited for the study (see Table 1 for characteristics of all 12 participants). Detailed information about the clinical characteristics of nine of the participants have been reported elsewhere[2]. The study conformed to the Declaration of Helsinki and was approved by the National Health Service Research Ethics Committee for Wales as well as the ethics committees of the School of Optometry and Vision Sciences, Cardiff University, and the Division of Optometry and Visual Science, City University, London. All participants provided their written consent after receiving a participant information sheet and having the opportunity to ask questions. Nine participants with ADOA (ID numbers 1010-1017, 1021) were examined in Cardiff and the rest at City University London by the same investigator.

Electroretinograms

Accepted 21-10-2015

All ERGs were recorded monocularly using a DTL fiber active electrode (Unimed Electrode Supplies, Ltd, Surrey, UK) and a contralateral reference. The DTL fiber was placed in the lower fornix to maximize stability during recording and the loose end fastened using medical tape at the inner canthus (Blenderm, Viasys Healthcare Ltd., Warwick, UK). A silver-silver chloride 10mm diameter touch-proof skin electrode (Unimed Electrode Supplies, Ltd, Surrey, UK), placed at the mid-frontal forehead position was used as ground electrode.

ERG responses were obtained using an evoked potential monitoring system (Medelec EP, Oxford Instruments PLC, Surrey, UK [Cardiff site]; Espion, Diagnosys LLC, Cambridge, UK [City University site]). Responses were bandpass filtered from 1 – 100 Hz and digitally averaged. Signals were recorded in blocks of 10 - 20 responses, with a total of 40 – 60 averaged per trace. Between 4 and 6 traces were obtained for each stimulus condition. The traces were superimposed to confirm signal repeatability and averaged off-line into a single averaged trace containing 160 – 300 responses. An automatic artefact rejection system removed signals contaminated by large eye movements and blinks.

Transient PERG stimuli (4 reversals per second; check size = 1^{o}) were generated on a computer monitor at 98% contrast. The screen was masked with a black opaque cardboard with a 13 x 13 cm square cut-out at the center so that it produced a 20^{o} x 20^{o} field at a viewing distance of 36cm.

Long duration ERGs were recorded using a red flash stimulus (peak output 660nm, 250msec duration, 3.33 log phot td, 2Hz) on a rod saturating blue background (peak

output 469nm, 3.49 scot log td) produced by a hand-held miniature Ganzfeld light emitting diode (LED) stimulator (CH Electronics, Kent, UK). Focal stimulation was produced by mounting the miniature Ganzfeld LED tube into the middle of a light box (44 cm x 44 cm x 10 cm) such that the circular stimulus subtended 20° diameter at a viewing distance of 15.6 cm. The 20° stimulus size was chosen to encompass as much of the central field as possible while avoiding the optic disc which starts about 12°-15° nasal to the fovea. In order to minimize the effect of stray light stimulating the peripheral retina (i.e. the area outside the stimulus area) the light box contained a strip of white LEDs (Super Bright InGan) passed through a blue filter (Lee Filter 068 Sky Blue, Lee Filters, Hampshire, UK) to produce a desensitizing blue surround of 3.73 scot log td (field size = 109° x 109° field). Cross hairs centered in the middle of the stimulus served as the fixation target. Full-field ERGs were recorded by holding the stimulator head, fitted with a diffusing cap, directly to the eye.

Full-field brief (flash) ERGs were elicited by a Ganzfeld stimulator (GS2000, LACE Elettronica, Italy) presenting a xenon flash stimulus (1.76 log td.s, 300 µsec maximum flash duration, 4Hz). Filters were used to obtain a red stimulus (Lee Filter "Terry Red", Lee Filters, Hampshire, UK, transmittance <5% at wavelengths shorter than 575 nm, and above 85% from 625–700 nm) over a continuous rod saturating 3.39 scot log td blue background (Schott Glass filter BG28, Schott AG, Mainz, Germany, peak transmittance 454 nm). All stimulus backgrounds were of sufficient scotopic illuminance to saturate the rods[35].

All ERGs were recorded by the same investigator using the same protocol at both sites. Long duration ERGs (focal and full-field) were generated by the same

miniature Ganzfeld LED stimulator at both sites. PERG and full-field brief flash data were only obtained from participants attending Cardiff University, in order to ensure consistency. All stimuli were calibrated using an ILT 1700 radiometer with SED033/Y/R luminance detector (Able Instruments and Controls, Reading, UK) assuming a 7 mm pupil with no correction for the Stiles-Crawford effect. The wavelength of the light sources were measured using a Specbos 1201 spectro-radiometer (Horiba Jobin Yvon Ltd, Middlesex, UK).

Procedures

All participants underwent a comprehensive ophthalmic examination which included best corrected visual acuity (ETDRS), contrast sensitivity (Pelli-Robson), visual field assessment (24-2 SITA-FAST, Humphrey Visual Field Analyzer), slit lamp biomicroscopy, optical coherence tomography (OCT; Topcon 3D-OCT 1000), fundus photography, color vision (D-15 desaturated test) and auto-refraction. In order to target earlier stage ADOA, the eye with the better visual field mean deviation score was selected for ERG recording, with the dominant eye chosen in the case of equal scores between the two eyes.

PERGs were always recorded first with natural pupils and near refractive correction when necessary. Pupils were then dilated using 1% tropicamide to a minimum of 7mm and flash ERGs were recorded in the following order: focal long-duration, full-field long duration and full-field brief flash ERG.

Signal Analysis

PERGs and focal ERGs were Fourier analyzed to remove high frequency noise above 30Hz and 50Hz respectively. The method for measuring the amplitude of the various sub-components is described in Figure 1. The $PhNR_{ON}$ (PhNR for brief flash ERG) and $PhNR_{OFF}$ amplitudes were measured from the pre-stimulus baseline and voltage at stimulus offset respectively to a fixed time point in their respective troughs. When determining the most appropriate fixed time point at which to measure the $PhNR_{ON}$ and $PhNR_{OFF}$ responses, the group averaged ERG of ADOA participants was subtracted from the group averaged ERG of the controls to obtain a difference ERG. The implicit time of the greatest discrepancy between the two was identified for the $PhNR_{ON}$ and $PhNR_{OFF}$ responses and was used as the fixed time point for all measurements. The fixed times at which the PhNR amplitudes were measured were as follows: focal $PhNR_{ON}$ at 95 msec after onset, focal $PhNR_{OFF}$ at 97 msec after offset, full-field $PhNR_{ON}$ at 83 msec after onset, full-field $PhNR_{OFF}$ at 102 msec after offset and full-field brief PhNR at 72 msec after onset. The identification of all peaks and troughs was determined objectively using Microsoft Excel i.e. as the minimum/maximum voltage within a fixed time window.

Statistical Analysis

Data expressed on a logarithmic scale (i.e. visual acuity, contrast sensitivity and visual field mean deviation) were converted (anti-logged) into a linear scale to calculate mean and standard deviation (SD) values. The mean and SD values were then converted back to log units. The distribution of the ERG data was checked for normality using the Shapiro-Wilk test. Where data were normally distributed, independent samples t-tests (2-tailed) were used to compare controls and participants with ADOA; the Mann-Whitney U test was used where data were non-

Accepted 21-10-2015

normally distributed. In order to minimize Type 1 errors due to the number of comparisons made (n = 35), we applied a Bonferroni adjustment to the alpha level (0.05) and report observations as significant when $p \leq 0.0014$. Receiver Operating Characteristic (ROC) curve analysis was used to calculate the area under the curve (AUC) to assess the diagnostic potential of the various ERG components. The comparison between AUCs were made using the method described by Hanley and McNeil (1983)[36].

Results

The clinical characteristics of all 12 ADOA participants from 6 families are shown in Table 1. The means and standard deviation for visual acuity, contrast sensitivity and mean deviation were 1.10 $\pm$ 1.07 logMAR, 1.30 $\pm$ 1.26 log units and -7.39 $\pm$ 7.09 dB respectively. The visual field defects were mostly central or centrocecal and color vision defects were variable but participants from the same family had similar defects. More details regarding the relationship between the clinical characteristics and ERG data in ADOA participants is to be the subject of a future manuscript.

Pattern ERGs

PERGs recorded from 9 ADOA participants are shown superimposed on the group averaged trace of 16 controls in the left hand column of Figure 2A. It shows that the negative N95 component is reduced in amplitude for all participants with ADOA, beyond the 95% confidence intervals for the control data. The P50 amplitudes in ADOA participants were also below the lower 95% confidence intervals except for one participant. The middle column of Figure 2A and the data in Table 2

demonstrate that the mean P50 and N95 amplitudes were significantly reduced in ADOA participants compared to controls. The mean N95:P50 ratio in ADOA participants of 1.05 was significantly reduced compared to 1.73 in controls (Table 2). Although there was evidence of P50 and N95 loss in people with ADOA, the difference plot in the right hand column of Figure 2A is dominated by a negative going signal corresponding to the loss of the N95 component.

Focal Long Duration Cone ERGs

Focal long duration cone ERGs recorded from 12 participants with ADOA are shown superimposed on the group averaged trace of 16 controls in the left column of Figure 2B. The typical ERG responses were characterized by the a-wave, b-wave, $PhNR_{ON}$, d-wave and $PhNR_{OFF}$. The $PhNR_{ON}$ was reduced in amplitude below the lower 95% confidence limit of the control data in almost all ADOA participants except one. Notably, the waveform after stimulus offset varied considerably between ADOA participants. For instance in participants with ADOA, the most prominent positive peak after stimulus offset, assumed to be the d-wave, was delayed and had a broad peak whose maximum amplitude occurred at highly variable times (Figure 2B, right and middle columns). In comparison, this prominent peak was highly consistent between control participants with respect to implicit time and was reflected in the much smaller standard deviation of the d-wave implicit time in controls than in participants with ADOA (Table 2).

The difference plot (Figure 2B, right) was dominated by two negative going waves representing the $PhNR_{ON}$ and $PhNR_{OFF}$ components affected by ADOA. The

difference plots of the ON and OFF components had similar profiles and amplitudes 2.80 µV and 2.88 µV respectively.

Long Duration Full-field Cone ERG

The long duration full-field cone ERGs in Figure 2C were recorded from the same ADOA participants (thin lines) and controls (group averaged thick black line) as the focal cone ERGs in Figure 2B. The form of the long duration ERG was similar under focal and full-field conditions with one exception. There were two positive peaks immediately after light offset in the full-field ERG; the first being the d-wave[24, 37]. The mean amplitude of the $PhNR_{OFF}$, but not the $PhNR_{ON}$, was significantly reduced in participants with ADOA (Table 2). On the difference plot (Figure 2C, right) the amplitude of the $PhNR_{OFF}$ difference (8.76 µV) was more than twice the amplitude of the $PhNR_{ON}$ difference (3.42 µV) when measured.

Once again, the OFF components showed greater variability than ON components for participants with ADOA. In fact, in at least 6 participants with ADOA, there was a third positive peak (3PP) after light offset not seen in controls (Figure 2C, left). There was no obvious pattern to the presence or absence of the 3PP in ADOA participants. The amplitude and implicit time of the 3PP measured from the ADOA group averaged trace was 13.34 µV and 75 msec after light offset respectively. Comparatively, none of the control traces displayed the 3PP prominently, although on close visual inspection, a kink corresponding in time with the 3PP was observed in some individual control traces.

Comparison of Focal and Full-field Long Duration ERGs

The waveform of the focal and full-field long duration ERGs was further compared by normalizing the group averaged ERGs to their respective b-wave amplitudes (Figure 3). The focal and full-field ERGs of controls (Figure 3A) and participants with ADOA (Figure 3B) had similar profiles although implicit times of the b-wave, $PhNR_{ON}$ and d-wave were significantly delayed in the focal ERG ($p \leq 0.01$, data not shown). The most prominent positive peak of the focal ERG after light offset coincided with the 2PP of the full-field ERG in the control traces while in the ADOA group, the broad peak of the focal ERG after offset described a curve that roughly matched the profile of the 2PP and 3PP of the full-field ERG.

In controls, the PhNRs are proportionally greater in the focal ERG than in the full-field ERG (Figure 3A). The losses in amplitudes of the PhNRs were also greater in the focal ERG than the full-field ERG in participants with ADOA (Figure 3B and 3C).

The Brief Full-field ERG

Brief full-field ERG recorded from 7 ADOA participants are shown in Figure 2D. Typical ERG responses had a-wave, b-wave, i-wave and PhNR components. The PhNR amplitude was reduced significantly in people with ADOA compared to controls (Figure 2D and Table 2). The difference plot in the right hand column of Figure 2D indicates that the greatest deficit in ADOA corresponds to the timing of the b-wave and the PhNR. An i-wave was recorded for all participants (controls and ADOA). Although it appeared more prominent in ADOA participants, there was no statistical difference in amplitude or implicit time between control and ADOA participants (Table 2).

Specificity and Sensitivity of the Different ERGs

Receiver operating characteristics (ROC) curves were used to determine the effectiveness of the N95 and long duration focal and full-field PhNRs at discriminating participants with ADOA from controls for 9 participants with ADOA and 16 controls for whom PERG and long duration focal and full-field ERG data were available (Figure 4). The AUC, sensitivity, specificity and cut off value which produced an optimal sensitivity while maintaining minimum specificity of ~90% are shown in Table 3. The N95 amplitude had the greatest diagnostic power. However, a comparison of the AUCs of the focal and full field PhNRs with the N95 amplitude, using the method described by Hanley and McNeil (1983)[36] showed that the N95 amplitude was only significantly more sensitive than the full-field $PhNR_{ON}$ amplitude ($z = 2.12$). Therefore, considered in terms of their diagnostic ability, the focal PhNRs and N95 component were not significantly different.

Discussion

Effect of ADOA on ON and OFF Retinal Ganglion Cells

In this study we sought to determine whether the $PhNR_{ON}$ was preferentially affected in ADOA as might be predicted based on the study by William et al[19]. Our findings however showed that in human patients, the $PhNR_{ON}$ and $PhNR_{OFF}$ amplitudes were equally reduced in the focal ERG, while in the full-field ERG, there was a greater reduction in the $PhNR_{OFF}$ amplitude than the $PhNR_{ON}$ amplitude. What then might explain this apparent contradiction?

Accepted 21-10-2015

336 In the study by William et al (2010), evidence for the preferential loss of ON-RGCs
337 was based on mouse retinal flat mounts showing significant dendritic pruning of ON-
338 but not OFF-RGCs. The experiment reported here however assessed the effect of
339 ADOA on the ON- and OFF-RGCs by evaluating the PhNR amplitude of the human
340 ERG, a functional measure. The role of the RGCs as primary originators of the
341 PhNR has been demonstrated by Frishman and colleagues[24-27, 34]. In experiments
342 using long duration full-field ERGs, they showed that that $PhNR_{ON}$ and $PhNR_{OFF}$
343 components were both reduced or eliminated after experimental glaucoma and
344 intravitreal injection of tetrodotoxin (TTX) (an agent that blocks generation of sodium
345 dependent spikes in retinal neurons) in macaque, as well as in patients with
346 glaucoma. Although, the origins of the $PhNR_{ON}$ and $PhNR_{OFF}$ have not been
347 conclusively traced to the ON- and OFF-RGCs respectively, Luo and Frishman[34]
348 showed that the $PhNR_{ON}$ (and b-wave) component but not the $PhNR_{OFF}$ (or d-wave)
349 was eliminated after injecting 2-amino-4-phosphonobutyric acid (APB) into the
350 macaque retina to block synaptic transmission from photoreceptors to ON-bipolar
351 cells and hence ON-RGCs. Injecting TTX after APB then removed the $PhNR_{OFF}$ but
352 not the d-wave thereby linking the $PhNR_{ON}$ and $PhNR_{OFF}$ components (although
353 indirectly) to the ON and OFF pathways respectively.
354
355 Previous human[31, 38, 39] and animal[24, 30] studies (including our mouse model) have
356 shown that the PhNR amplitude is very susceptible to RGC damage with severe
357 attenuation of PhNR amplitude recorded even when morphologic and other
358 functional parameters were within normal range i.e. in early stage disease. It is
359 possible that the $PhNR_{ON}$ pathways may be selectively compromised at an earlier
360 stage of the disease process than that studied here. A similar study in pre-

symptomatic people with the *OPA1* mutations or in people with ADOA at a much earlier stage of the disease (e.g. children with ADOA) could provide additional insights.

Our findings may also be a reflection of the heterogeneous nature of ADOA. There are over 200 *OPA1* mutations[15, 16] which cause ADOA with wide phenotypic variations both within and between affected families [2, 40]. Genotype-phenotype correlations have been difficult to establish in previous studies [3, 41] and the number of patients in each family of *OPA1* mutations (except Family E) was insufficient to reliably explore such correlations. In the mouse model, the mutant mice (>10 months old) were genetically homogenous and disease severity correlated with age. Participants studied here were from 6 families, with a different mutation in each family (Table 1), and at different stages of the disease. This may have diluted observations that would have been made from a homogenous cohort.

Comparison of Focal and Full-field PhNRs

The long duration focal and full-field ERGs in this study were recorded using the same stimulus parameters, which were comparable to the parameters recommended by Kondo et al[42] for eliciting focal responses. Although the waveforms of the focal and full field ERGs were similar, they were not identical (Figure 3A-B). There was a greater contribution of $PhNR_{ON}$ and $PhNR_{OFF}$ components to the focal ERG than to the full-field ERG (Figure 3A) which reflects the decreasing proportion of RGCs to other retinal cells with eccentricity[43]. The focal PhNRs were more severely affected than their full-field counterparts by ADOA and this was reflected in the larger AUCs found for the focal signals. These findings were consistent with the central field

386 defects recorded in ADOA participants in this study and in others[2, 6, 44]. In addition,
387 whereas the focal PhNRs were both significantly reduced ($p<0.001$), only the full-
388 field $PhNR_{OFF}$ was significantly reduced in the full-field ERG (Table 2). Although the
389 N95 and focal PhNR amplitudes were highly discriminatory for ADOA, it should be
390 noted that the participants in this study had relatively late stage disease.
391
392 The symmetrical loss in the focal $PhNR_{ON}$ and $PhNR_{OFF}$ amplitudes (Figure 2B right
393 column and Figure 3C) may reflect the 1:1 ratio of ON- to OFF-RGCs in the macula,
394 while the greater loss in the full-field $PhNR_{OFF}$ amplitude than the $PhNR_{ON}$ amplitude
395 (Figure 2C right column and Figure 3C) may reflect the nearly 1:2 ratio of ON- to
396 OFF-RGCs in the peripheral retina [45-47]. The broadening of the d-wave peak in the
397 focal ERG and the presence of the 3PP in the full-field long ERG in participants with
398 ADOA may be due to contributions from the cone receptor potential (CRP) and/or
399 depolarizing OFF-bipolar cell responses after light offset which were unmasked in
400 the relative absence of the negative going $PhNR_{OFF}$ [48-50]. The 2PP may be the i_{OFF}-
401 wave described by Horn et al (2011)[51], although in contrast to their results, this study
402 did not record a significant difference in amplitude between controls and participants
403 with ADOA.
404
405 ***Comparison to other Electrophysiological Studies in ADOA***
406 Miyata et al[29] reported a significant reduction in the full-field brief PhNR, but none in
407 the a- or b-wave amplitude, in ADOA patients using white-on-white stimulus. Similar
408 results were obtained by Barnard et al[30] in the mouse model. In this present study,
409 we show similar results using a red on blue stimulus. The flash luminance used in
410 this study was adopted from a previous study in this laboratory[52] and was

Accepted 21-10-2015

411 comparable to the flash luminance used by Miyata et al[29]. This supports findings that
412 the red-on blue stimulus is effective for clinical evaluation of RGC function.
413
414 Holder et al[33] reported a significant reduction in N95 amplitude and the N95:P50 ratio
415 of the PERG participants with ADOA. We obtained similar results and showed that
416 the focal PhNRs and N95 amplitude were equally effective at discriminating controls
417 from participants with ADOA. The focal ERG could therefore be used as an
418 alternative to the PERG.
419
420 In this study, as well as in that of Holder et al[33], the P50 amplitude was significantly
421 reduced. This may indicate that bipolar cell function is compromised in ADOA as has
422 been put forward by Reis et al[53]. However, a reduction in P50 amplitude is also seen
423 when only RGCs are compromised[34], therefore the P50 reduction observed in this
424 study could be due to dysfunction of bipolar cells, RGCs or both.
425
426 **Conclusion**
427 This study showed there was a nearly symmetrical reduction in the $PhNR_{ON}$ and
428 $PhNR_{OFF}$ amplitudes in participants with ADOA with no evidence of a preferential
429 ON-pathway loss. This suggests that ON- and OFF-RGCs may be equally affected in
430 patients. In addition, in terms of their diagnostic potential, the focal PhNR-ON and -
431 OFF amplitudes were better than their full-field counterparts and were not
432 significantly different from the N95 amplitude of the PERG**.**
433
434 **Acknowledgement**

Accepted 21-10-2015

435 EM is funded by the Ghana Education Trust Fund. We acknowledge Fight for Sight
436 Small Grants Award (MV), for their contribution to genotyping.

REFERENCES

1. Marmor MF, Brigell MG, McCulloch DL, Westall CA, Bach M. ISCEV standard for clinical electro-oculography (2010 update). *Documenta Ophthalmologica* 2011;122:1-7.
2. Votruba M, Fitzke FW, Holder GE, Carter A, Bhattacharya SS, Moore AT. Clinical features in affected individuals from 21 pedigrees with dominant optic atrophy. *Arch Ophthalmol* 1998;116:351-358.
3. Votruba M, Thiselton D, Bhattacharya SS. Optic disc morphology of patients with OPA1 autosomal dominant optic atrophy. *Br J Ophthalmol* 2003;87:48-53.
4. Newman NJ, Biousse V. Hereditary optic neuropathies. *Eye* 2004;18:1144-1160.
5. Yu-Wai-Man P, Griffiths PG, Hudson G, Chinnery PF. Inherited mitochondrial optic neuropathies. *J Med Genet* 2009;46:145-158.
6. Votruba M, Moore AT, Bhattacharya SS. Clinical features, molecular genetics, and pathophysiology of dominant optic atrophy. *J Med Genet* 1998;35:793-800.
7. Krill AE, Smith VC, Pokorny J. Similarities between congenital tritan defects and dominant optic-nerve atrophy - coincidence or identity *J Opt Soc Am* 1970;60:1132-&.
8. Kjer B, Eiberg H, Kjer P, Rosenberg T. Dominant optic atrophy mapped to chromosome 3q region .2. Clinical and epidemiological aspects. *Acta Ophthalmol Scand* 1996;74:3-7.
9. Votruba M, Aijaz S, Moore AT. A review of primary hereditary optic neuropathies. *J Inherit Metab Dis* 2003;26:209-227.
10. Yu-Wai-Man P, Griffiths PG, Burke A, et al. The prevalence and natural history of dominant optic atrophy due to OPA1 mutations. *Ophthalmology* 2010;117:1538-1546, 1546.e1531.
11. Gallus GN, Cardaioli E, Rufa A, et al. High frequency of OPA1 mutations causing high ADOA prevalence in south-eastern Sicily, Italy. *Clin Genet* 2012;82:277-282.
12. Lenaers G, Hamel C, Delettre C, et al. Dominant optic atrophy. *Orphanet J Rare Dis* 2012;7.
13. Alexander C, Votruba M, Pesch UEA, et al. OPA1, encoding a dynamin-related GTPase, is mutated in autosomal dominant optic atrophy linked to chromosome 3q28. *Nat Genet* 2000;26:211-215.
14. Delettre C, Lenaers G, Griffoin JM, et al. Nuclear gene OPA1, encoding a mitochondrial dynamin-related protein, is mutated in dominant optic atrophy. *Nat Genet* 2000;26:207-210.
15. Ferre M, Bonneau D, Milea D, et al. Molecular Screening of 980 Cases of Suspected Hereditary Optic Neuropathy with a Report on 77 Novel OPA1 Mutations. *Hum Mutat* 2009;30:E692-E705.
16. Ferre M, Amati-Bonneau P, Tourmen Y, Malthiery Y, Reynier P. eOPA1: An online database for OPA1 mutations. *Hum Mutat* 2005;25:423-428.
17. Johnston PB, Gaster RN, Smith VC, Tripathi RC. A clinicopathologic study of autosomal dominant optic atrophy. *Am J Ophthalmol* 1979;88:868-875.
18. Kjer P, Jensen OA, Klinken L. Histopathology of eye, optic-nerve and brain in a case of dominant optic atrophy. *Acta Ophthalmol (Copenh)* 1983;61:300-312.
19. Williams PA, Morgan JE, Votruba M. Opa1 deficiency in a mouse model of dominant optic atrophy leads to retinal ganglion cell dendropathy. *Brain* 2010;133:2942-2951.

20. Sarzi E, Angebault C, Seveno M, et al. The human OPA1delTTAG mutation induces premature age-related systemic neurodegeneration in mouse. *Brain* 2012;135:3599-3613.
21. Alavi MV, Bette S, Schimpf S, et al. A splice site mutation in the murine Opa1 gene features pathology of autosomal dominant optic atrophy. *Brain* 2007;130:1029-1042.
22. Davies VJ, Hollins AJ, Piechota MJ, et al. Opa1 deficiency in a mouse model of autosomal dominant optic atrophy impairs mitochondrial morphology, optic nerve structure and visual function. *Hum Mol Genet* 2007;16:1307-1318.
23. Williams PA, Piechota M, von Ruhland C, Taylor E, Morgan JE, Votruba M. Opa1 is essential for retinal ganglion cell synaptic architecture and connectivity. *Brain* 2012;135:493-505.
24. Viswanathan S, Frishman LJ, Robson JG, Harwerth RS, Smith EL, 3rd. The photopic negative response of the macaque electroretinogram: reduction by experimental glaucoma. *Invest Ophthalmol Vis Sci* 1999;40:1124-1136.
25. Viswanathan S, Frishman LJ, Robson JG. The uniform field and pattern ERG in macaques with experimental glaucoma: removal of spiking activity. *Invest Ophthalmol Vis Sci* 2000;41:2797-2810.
26. Viswanathan S, Frishman LJ, Robson JG, Walters JW. The photopic negative response of the flash electroretinogram in primary open angle glaucoma. *Invest Ophthalmol Vis Sci* 2001;42:514-522.
27. Rangaswamy NV, Shirato S, Kaneko M, Digby BI, Robson JG, Frishman LJ. Effects of Spectral Characteristics of Ganzfeld Stimuli on the Photopic Negative Response (PhNR) of the ERG. *Invest Ophthalmol Vis Sci.* United States; 2007:4818-4828.
28. Sustar M, Hawlina M, Brecelj J. ON- and OFF-response of the photopic electroretinogram in relation to stimulus characteristics. *Doc Ophthalmol* 2006;113:43-52.
29. Miyata K, Nakamura M, Kondo M, et al. Reduction of oscillatory potentials and photopic negative response in patients with autosomal dominant optic atrophy with OPA1 mutations. *Invest Ophthalmol Vis Sci* 2007;48:820-824.
30. Barnard AR, Issa PC, Perganta G, et al. Specific deficits in visual electrophysiology in a mouse model of dominant optic atrophy. *Exp Eye Res* 2011;93:771-777.
31. Machida S, Tamada K, Oikawa T, et al. Comparison of photopic negative response of full-field and focal electroretinograms in detecting glaucomatous eyes. *Journal of ophthalmology* 2011;2011.
32. Tamada K, Machida S, Yokoyama D, Kurosaka D. Photopic negative response of full-field and focal macular electroretinograms in patients with optic nerve atrophy. *Jpn J Ophthalmol* 2009;53:608-614.
33. Holder GE, Votruba M, Carter AC, Bhattacharya SS, Fitzke FW, Moore AT. Electrophysiological findings in dominant optic atrophy (DOA) linking to the OPA1 locus on chromosome 3q 28-qter. *Doc Ophthalmol* 1998;95:217-228.
34. Luo X, Frishman LJ. Retinal Pathway Origins of the Pattern Electroretinogram (PERG). *Invest Ophthalmol Vis Sci* 2011;52:8571-8584.
35. Aguilar M, Stiles WS. Saturation of the rod mechanism of the retina at high levels of stimulation. *Opt Acta (Lond)* 1954;1:59-65.
36. Hanley JA, McNeil BJ. A method of comparing the areas under receiver operating characteristic curves derived from the same cases. *Radiology* 1983;148:839-843.

37. Evers HU, Gouras P. Three cone mechanisms in the primate electroretinogram: two with, one without off-center bipolar responses. *Vision Res* 1986;26:245-254.
38. Nakamura H, Miyamoto K, Yokota S, Ogino K, Yoshimura N. Focal macular photopic negative response in patients with optic neuritis. *Eye (Lond)* 2011:358-364.
39. Gotoh Y, Machida S, Tazawa Y. Selective loss of the photopic negative response in patients with optic nerve atrophy. *Arch Ophthalmol* 2004:341-346.
40. Granse L, Bergstrand I, Thiselton D, et al. Electrophysiology and ocular blood flow in a family with dominant optic nerve atrophy and a mutation in the OPA1 gene. *Ophthalmic Genet* 2003;24:233-245.
41. Yu-Wai-Man P, Griffiths PG, Gorman GS, et al. Multi-system neurological disease is common in patients with OPA1 mutations. *Brain* 2010;133:771-786.
42. Kondo M, Kurimoto Y, Sakai T, et al. Recording focal macular photopic negative response (PhNR) from monkeys. *Invest Ophthalmol Vis Sci* 2008:3544-3550.
43. Curcio CA, Allen KA. Topography of ganglion-cells in human retina. *J Comp Neurol* 1990;300:5-25.
44. Fuhrmann N, Schimpf S, Kamenisch Y, et al. Solving a 50 year mystery of a missing OPA1 mutation: more insights from the first family diagnosed with autosomal dominant optic atrophy. *Mol Neurodegener* 2010;5.
45. Dacey DM, Petersen MR. Dendritic field size and morphology of midget and parasol ganglion-cells of the human retina. *Proc Natl Acad Sci U S A* 1992;89:9666-9670.
46. Dacey DM. The mosaic of midget ganglion cells in the human retina. *J Neurosci* 1993;13:5334-5355.
47. Drasdo N, Millican CL, Katholi CR, Curcio CA. The length of Henle fibers in the human retina and a model of ganglion receptive field density in the visual field. *Vision Res* 2007;47:2901-2911.
48. Bush RA, Sieving PA. A proximal retinal component in the primate photopic ERG a-wave. *Invest Ophthalmol Vis Sci* 1994;35:635-645.
49. Ueno S, Kondo M, Ueno M, Miyata K, Terasaki H, Miyake Y. Contribution of retinal neurons to d-wave of primate photopic electroretinograms. *Vision Res* 2006;46:658-664.
50. Sieving PA, Murayama K, Naarendorp F. Push-pull model of the primate photopic electroretinogram: a role for hyperpolarizing neurons in shaping the b-wave. *Vis Neurosci* 1994;11:519-532.
51. Horn FK, Gottschalk K, Mardin CY, Pangeni G, Junemann AG, Kremers J. On and off responses of the photopic fullfield ERG in normal subjects and glaucoma patients. *Doc Ophthalmol* 2011;122:53-62.
52. Mortlock KE, Binns AM, Aldebasi YH, North RV. Inter-subject, inter-ocular and inter-session repeatability of the photopic negative response of the electroretinogram recorded using DTL and skin electrodes. *Doc Ophthalmol* 2010;121:123-134.
53. Reis A, Mateus C, Viegas T, et al. Physiological evidence for impairment in autosomal dominant optic atrophy at the pre-ganglion level. *Graefes Arch Clin Exp Ophthalmol* 2013;251:221-234.

583 **FIGURES AND TABLES**

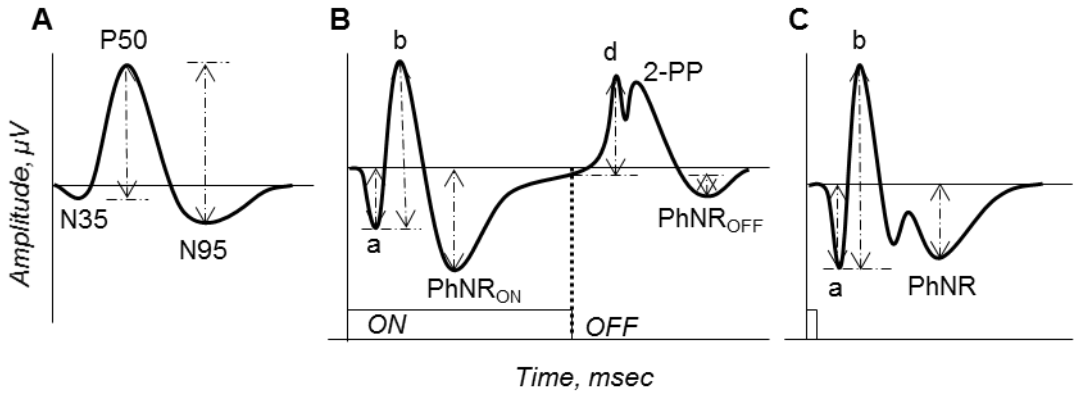

Figure 1. Representative ERG traces of the (A) PERG, (B) full-field long-duration ERG and (C) full-field brief flash ERG showing their components and how their amplitudes were measured (double headed arrows). The amplitudes of the P50, N95 (A), a-wave (*a*) and b-wave *(b)* (B-C) were measured as recommended by the International Society of Clinical Electrophysiology of Vision (ISCEV)[1]. The d-wave (*d*) amplitude was measured from the point of light offset to the peak of the d-wave. The $PhNR_{ON}$ (PhNR in brief flash) and $PhNR_{OFF}$ amplitudes were measured from the pre-stimulus baseline and voltage at stimulus offset respectively to a fixed time point in their respective troughs (see main text for details). The focal long duration ERG had the same profile as the full-field long duration except that in the focal ERG there was only one prominent positive peak after light offset, the d-wave.

584

585

586 Table 1. Clinical Characteristics of Participants with ADOA

Participant ID/Gender	Family	Age	Visual Acuity, logMAR		Contrast Sensitivity, log units		Mean Deviation, dB		Color Vision	*OPA1* Mutation
			RE	LE	RE	LE	RE	LE		
1010/F	A	49	1.34	1.32	0.35	0.40	-27.03	-25.15	Mixed	c.1202G>A
1011/F	B	55	1.64	1.62	0.00	0.00	-17.65	-19.58	Mixed	C1508A
1012/F	C	58	0.80	1.00	1.15	1.05	-8.68	-10.39	Mixed	IVS8+5G>A
1013/F	C	61	1.10	0.64	NA	NA	-12.47	-9.06	Mixed	IVS8+5G>A
1014/M	D	33	1.40	1.32	0.30	0.45	-13.84	-11.89	Protan/ Deutan	NA
1015/F	D	31	1.02	0.98	1.05	1.05	-13.98	-13.20	Protan/ Deutan	NA
1016/F	E	18	0.80	0.80	1.65	1.35	-7.08	-8.15	Tritan	IVS9+3A>T
1017/F	E	27	0.82	0.80	1.65	1.65	-5.14	-5.82	Tritan	IVS9+3A>T
1018/F	E	59	0.86	0.96	0.90	0.75	-9.55	-7.03	Tritan	IVS9+3A>T
1019/F	E	49	0.72	1.20	1.50	1.50	-5.99	-6.79	Tritan	IVS9+3A>T
1020/M	E	46	0.98	1.20	1.65	1.20	-10.15	-8.21	Tritan	IVS9+3A>T
1021/M	F	39	0.02	0.00	1.65	1.65	-1.31	-2.25	NA	c.357delT

587 NA – Not available

Accepted 21-10-2015

588

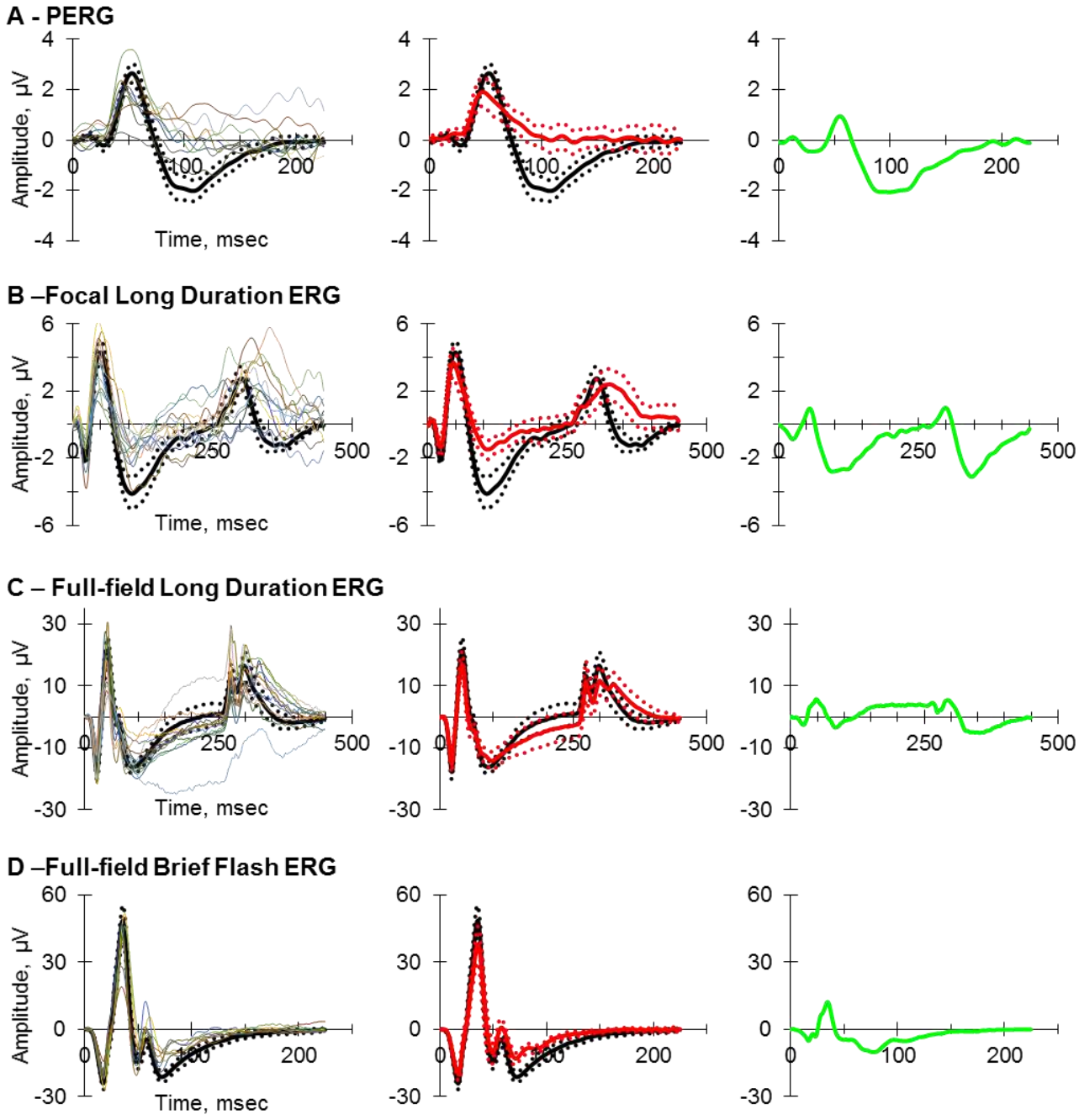

589

Figure 2. ERG traces of the (A) PERG, (B) focal long duration ERG, (C) full-field long duration ERG and (D) full-field brief flash ERG recorded from participants in this study. Left column: individual traces of participants with ADOA (thin lines) superimposed on the group averaged ERG of 16 controls (thick lines) for each type of ERG recorded. The number of participants with ADOA in A, B, C and D are 9, 12, 12 and 7 respectively. Dotted lines represent 95% confidence intervals. Middle column: comparison between group-averaged traces of controls (thick black line) and ADOA participants (thick red line). Right column: difference plots generated by subtracting the group-averaged ADOA ERG from the control ERG.

Accepted 21-10-2015

590 Table 2. Means of Amplitudes and Implicit Times in Controls and Participants with ADOA

ERG TYPE	Component		ADOA Mean Values	Control Mean Values	P-value
PERG	P50	A, µV	1.92 ± 0.81	3.18 ± 0.81	0.0011*
		T, msec	49.03 ± 3.67	53.16 + 3.28	0.0082
	N95	A, µV	2.12 ± 1.31	5.20 ± 0.87	0.0000*
		T, msec	101.67 ± 11.21	99.77 ± 7.76	0.6212†
	N95:P50 Ratio		1.05 ± 0.31	1.73 ± 0.47	0.0009*†
Focal ERG	a-wave	A, µV	1.76 ± 0.94	2.22 ± 0.61	0.1301
		T, msec	23.00 ± 1.72	23.75 + 1.74	0.2534
	b-wave	A, µV	5.29 ± 2.08	6.76 ± 1.74	0.0524
		T, msec	46.25 + 3.14	49.81 + 4.88	0.0271
	$PhNR_{ON}$	A, µV	1.02 ± 0.97	3.81 ± 1.74	0.0000*
		T, msec	109.25 ± 7.16	104.50 ± 8.49	0.1299
	d-wave	A, µV	2.81 ± 1.52	3.12 ± 1.04	0.5290
		T, msec	321.92 ± 13.80	302.41 ± 5.92	0.0004*
	$PhNR_{OFF}$	A, µV	-1.97 ± 1.52	0.93 ± 1.23	0.0000*
		T, msec	138.08 + 9.94	113.09 + 14.64	0.0000*†
Full-field Long ERG	a-wave	A, µV	15.87 ± 4.44	18.84 ± 4.45	0.0917
		T, msec	22.50 ± 1.09	23.16 ± 1.70	0.2537
	b-wave	A, µV	33.57 ± 10.67	41.29 ± 11.18	0.0768
		T, msec	41.83 ± 2.86	42.16 ± 2.47	0.7515
	$PhNR_{ON}$	A, µV	12.26 ± 3.95	15.68 ± 4.36	0.0430
		T, msec	96.18 + 9.16	92.72 + 4.15	0.2471
	d-wave	A, µV	15.11 ± 6.20	12.84 ± 4.89	0.2866
		T, msec	274.67 ± 1.15	273.47 ± 1.02	0.0075†
	2^{nd} positive peak	A, µV	15.48 ± 4.87	16.10 ± 7.55	0.8064
		T, msec	302.50 ± 8.35	298.19 ± 2.00	0.1054†
	$PhNR_{OFF}$	A, µV	-8.31 ± 5.69	0.45 ± 5.74	0.0005*
		T, msec	178.33 + 27.02	132.19 + 17.30	0.0000*†
Full-field Brief ERG	a-wave	A, µV	20.60 ± 3.79	25.73 ± 5.91	0.0480†
		T, msec	17.50 ± 0.69	17.22 ± 0.76	0.4133
	b-wave	A, µV	59.75 + 14.58	77.88 ± 18.17	0.0302
		T, msec	35.39 ± 1.51	35.38 ± 1.26	0.9767
	i-wave	A, µV	14.00 ± 8.37	16.19 ± 7.58	0.5420
		T, msec	58.04 ± 2.04	57.61 ± 2.37	0.6844
	PhNR	A, µV	12.93 ± 3.38	22.39 ± 6.17	0.0011*
		T, msec	72.75 + 4.13	70.59 + 6.40	0.4244†

591 Data are expressed as mean ± standard deviation.
592 A – Amplitude; T – Implicit time from stimulus onset
593 * – Value is significant at $p \leq 0.0014$ level; † – data was non-uniformly distributed and Mann-Whitney
594 U test was used for statistical comparison.
595

Accepted 21-10-2015

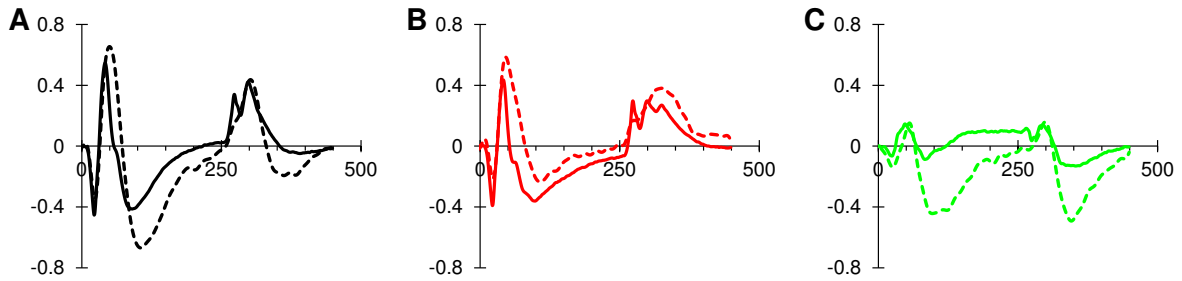

Figure 3. A comparison of the long duration focal (dashed lines) and full field (solid lines) group-averaged ERGs for (A) controls, (B) participants with ADOA and (C) difference plots. ERGs have been normalised to the b-wave amplitude of their respective control group-averaged ERG.

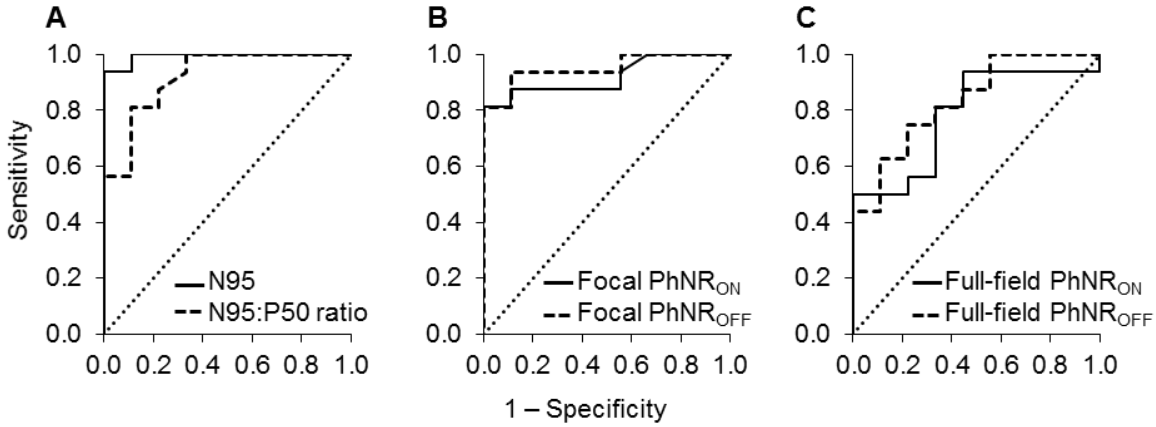

Figure 4. Receiver Operating Characteristic (ROC) curves derived using (A) N95 component and N95:P50 ratio of the PERG, (B) focal PhNR$_{ON}$ and PhNR$_{OFF}$ amplitudes and (C) full-field PhNR$_{ON}$ and PhNR$_{OFF}$ amplitudes. Diagonal dashed line is the reference line.

Table 3. Sensitivity, Specificity and Area Under Curve of ROC Analysis for ERG Components

Test Variable	Area (95% CI)	Sensitivity	Specificity	Cut Off Value
N95	0.99 (0.97 – 1.00)	93.80	100.00	4.12 µV
N95:P50	0.92 (0.81 – 1.00)	81.30	89.90	1.44
Focal PhNR$_{ON}$	0.92 (0.81 – 1. 00)	81.30	100.00	2.62 µV
Focal PhNR$_{OFF}$	0.95 (0.87 – 1.00)	81.30	100.00	0.24 µV
Full-field PhNR$_{ON}$	0.78 (0.60 – 0.97)	50.00	100.00	16.99 µV
Full-field PhNR$_{OFF}$	0.83 (0.73 – 0.99)	62.50	89.90	0.35 µV

Accepted 21-10-2015